4-Diazinyl- and 4-Pyridinylimidazoles: Potent Angiotensin II Antagonists. A Study of Their Activity and Computational Characterization

Nicholas, J. S. Harmat,*,† Raffaello Giorgi,† Fabrizio Bonaccorsi,† Guido Cerbai,† Spartaco M. Colombani,† Anna R. Renzetti,† Rocco Cirillo,† Alessandro Subissi,† Giuliano Alagona,‡ Caterina Ghio,‡ Federico Arcamone,§ Antonio Giachetti,§ Fabio Paleari,⊥ and Aldo Salimbeni⊥

Departments of Medicinal Chemistry and Pharmacology, Laboratori Guidotti S.p.A., Via Livornese 897, 56122 S. Piero a Grado, Pisa, Italy, CNR-Istituto di Chimica Quantistica ed Energetica Molecolare,Via Risorgimento 35, 56126 Pisa, Italy, A. Menarini Industrie Farmaceutiche Riunite s.r.l., Via Sette Santi 3, 50131 Firenze, Italy, and Medicinal Chemistry Department, Istituto Lusofarmaco, 20132 Milano, Italy

Received April 13, 1995®

A series of *N*-[biphenylyl(tetrazolyl)methyl]-2-butylimidazoles containing variously substituted diazine or pyridine moieties either as their free bases or *N*-oxide derivatives attached to the 4-position of the imidazole ring was synthesized and tested for interaction with the AT_1 receptors of rat adrenal cortex membranes (receptor binding assay). Some compounds were then chosen for further evaluation *in vivo* in the A II-induced pressor response in conscious normotensive rats. The most potent in the AT_1 binding assay were found to be compounds in which the diazine or pyridine ring nitrogen is adjacent to the point of attachment between the two heteroaromatic rings such as 2-butyl-4-(3,6-dimethylpyrazin-2-yl)-1-[[2′-(1*H*-tetrazol-5-yl)-biphenyl-4-yl]methyl]-1*H*-imidazole (**3b**) or 2-butyl-4-[5-(methoxycarbonyl)pyrid-2-yl]-1-[[2′-(1*H*-tetrazol-5-yl)biphenyl-4-yl]methyl]-1*H*-imidazole (**6c**). The binding affinities and oral activities of the pyridine *N*-oxide imidazoles in which a stabilizing group ortho to the pyridine ring nitrogen is present were markedly improved as in 2-butyl-4-[(3-methoxycarbonyl)-6-methyl-*N*-oxopyridin-2-yl]-1-[[2′-(1*H*-tetrazol-5-yl)biphenyl-4-yl]methyl]-1*H*-imidazole **31b**. Molecular modeling studies were carried out to determine the molecular electrostatic potential values of related model systems and to correlate their receptor interaction energies with the observed activities of our compounds.

The blocking of the renin–angiotensin system (RAS) with angiotensin-converting enzyme (ACE) inhibitors has been shown to be effective in the control of hypertension and congestive heart failure. On the basis of the effectiveness of ACE inhibitors in cardiovascular control, there has been intense activity in the discovery of oral angiotensin II (A II) antagonists as a means of inhibiting the RAS, with the hope of obtaining greater pharmacological selectivity than observed with ACE inhibitors.

Following the initial lead by Takeda in the development of non-peptide A II antagonists, where it was reported that the imidazole compound (**1a**, Figure 1) possessed weak activity,[1] there has been a lot of effort directed toward developing A II antagonists based on a variety of N-heterocyclic systems over the years. DuPont prepared a series of compounds linking the imidazole to a biphenylyltetrazole (BPT) moiety, leading to the development of the orally active DuP 753 (losartan **1b**).[2] Subsequently, there have been many other reports of A II antagonists consisting of an alkyl-substituted heterocycle connected to the BPT unit,[3–7] and also other classes of nitrogen compounds containing the BPT group but not related to imidazole structure have also been discovered to be potent A II antagonists.[8–11] There are at least two distinct angiotensin II receptor subtypes, designated as AT_1 and AT_2. Losartan is selective for the AT_1 site, which mediates most of the known angiotensin II physiological functions, such as vasoconstriction.

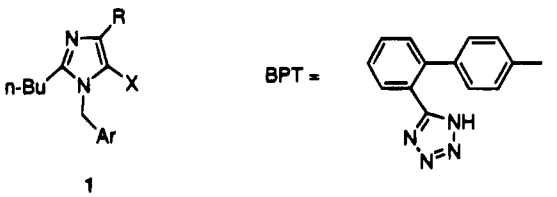

1

1a R = Cl, X = CH_2CO_2H, Ar = 2-Cl-Ph (Takeda)
1b R = Cl, X = CH_2OH, Ar = BPT (DuPont)
1c R = Cl, X = CO_2H, Ar = BPT
1d R = C_2F_5, X= CO_2H, Ar = BPT

Figure 1.

In our work we chose to focus on 2-*n*-butyl-4-heteroarylimidazole systems corresponding to general structure **2** containing various diazinyl (structures **3**–**5**) and pyridinyl heterocycle systems (structure **6**) as A II antagonists for the AT_1 receptor site (Figure 2). On the basis of the structure–activity relationships of non-peptide A-II antagonists,[12a] the BPT imidazole-containing structures provide maximum potency by interaction with three lipophilic pockets of the AT_1 receptor site one of these interactions being provided by the presence of electronegative and lipophilic substituents at the 4-position of the imidazole ring.[12b,c] It was thought that substitution of the chlorine in Dup 753 with electron-deficient heteroaromatic moieties leading to the conjugated bis-heteroaryl system **2** could produce compounds with potent A II antagonistic activity, by the heteroaromatic ring fitting into one of these lipophilic regions of the receptor site in place of the halogen. The idea was

* Author to whom correspondence should be addressed.
† Laboratori Guidotti, S.p.A., Pisa.
‡ CNR Istituto di Chimica Quantistica ed Energetica Molecolare, Pisa.
§ A. Menarini Industrie Farmaceutiche Riunite s.r.l., Firenze.
⊥ Medicinal Chemistry Department, Istituto Lusofarmaco, Milano.
® Abstract published in *Advance ACS Abstracts,* June 15, 1995.

0022-2623/95/1838-2925$09.00/0

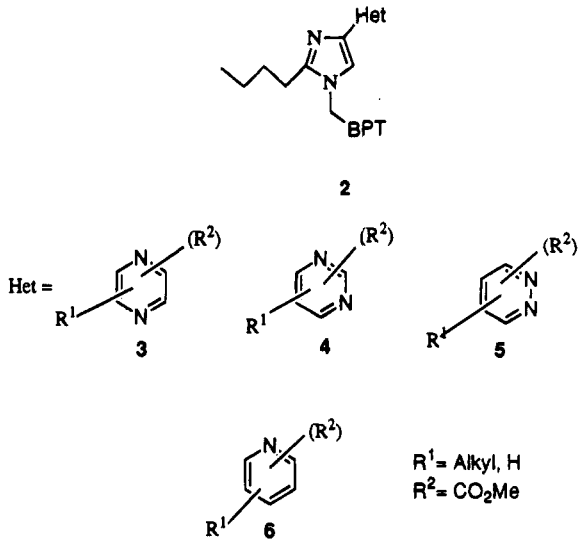

Figure 2.

that heteroatoms (like nitrogen) in the heteroaromatic rings might play a role similar to that of the hydroxymethyl group in the 5-position of the imidazole ring of **1b**. Also examined was the effect on binding of these molecules to the A II receptor site by the nature and position of various substituents attached to the diazine or pyridine rings.

Chemistry

The series of 2-*n*-butyl-4-heteroarylimidazole compounds with the BPT group attached to N-1 of the imidazole ring (**3**–**6**) was obtained as depicted in Scheme 1. Starting from N-1-protected SEM imidazole **8**, the lithiation of the 2-position of the imidazole ring in **8** followed by alkylation with butyl iodide gave **9**. A further second regioselective lithiation of **9** and subsequent reaction with tributyltin chloride as previously described[13] furnished the stannylimidazole derivative **10**. The coupling of **10** with various diazinyl or pyridinyl halides (Het-X, X = Cl, Br, I)[14–21] was accomplished in the presence of the tetrakis(triphenylphosphine)-palladium(0) catalyst in refluxing dioxane to yield the coupled products (**11**–**14**). The removal of SEM protecting group in the intermediates (**11**–**14**) was carried out by two methods depending on the type of substituent attached to the diazine or pyridine portion of the molecule (Tables 1 and 2, compounds **3**–**6**). For hydrolytically nonsensitive groups where R_1 and/or R_2 = alkyl, the removal of the SEM protecting group was carried out by refluxing in 5 N aqueous HCl. For compounds bearing hydrolytically sensitive groups, namely where R_1 or R_2 = CO_2Me, the deprotection was carried out using anhydrous HCl in methanol. The resulting deprotected imidazoles (**15**–**18**) were then N-alkylated with the trityl-protected derivative of BPT **23** to give the products **19**–**22**. It was anticipated at this stage that a mixture of regioisomers would have been obtained on the N-alkylation of compounds **15**–**18**. However, in all cases only one regioisomer was found to be formed as evidenced by the ^{1}H-NMR characterization of **19**–**22**, this being attributed to the steric bulk of the diazinyl or pyridinyl group directing alkylation to one of the nitrogens of the imidazole ring. Detritylation of compounds **19**–**22** by refluxing in methanol furnished the final target compounds **3**–**6** (Tables 1 and 2).

Scheme 1[a]

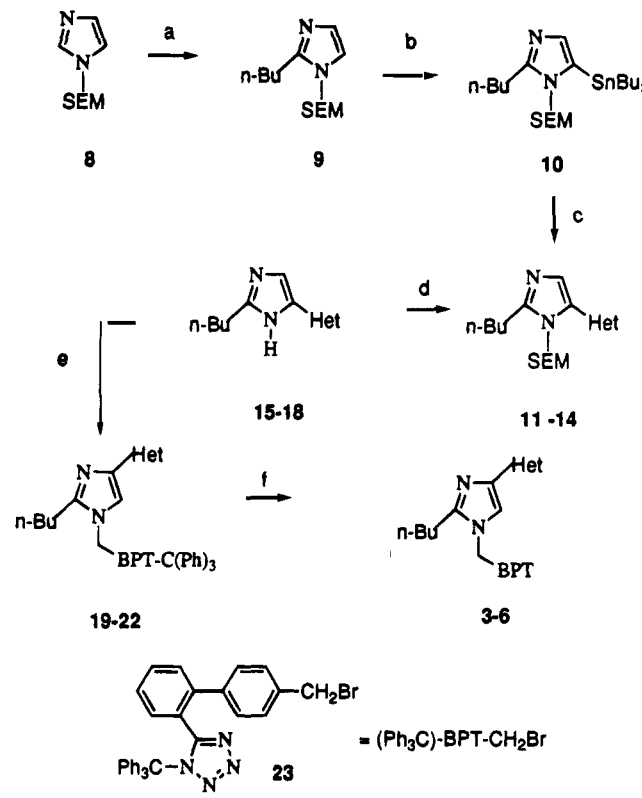

[a] (a) BuLi/TMEDA/*n*-BuI; (b) BuLi/Et_2O/*n*-Bu_3SnCl; (c) Het-X (X = Cl, Br, I), $Pd(PPh_3)_4$, dioxane, reflux; (d) method A. 5 N HCl, H_2O, MeOH, reflux or method B: dry HCl(g); (e) NaH/DMF (Ph_3C)BPT-CH_2Br (**23**); (f) MeOH, reflux.

Two-dimensional NMR NOESY experiments were carried out on some of the final 2-pyridinyl and 3-pyridinyl and one of the pyrazine compounds in the series to obtain information about the relative position of the heterocyclic ring with respect to the imidazole. In all the compounds examined, a strong cross peak was observed between the benzylic protons of the BPT group and the proton in position 5 of the imidazole ring, indicating that the pyridinyl or diazinyl moiety is attached to position 4 of the imidazole ring, so confirming their structures to be that of the general structure **2**. Also, the trace corresponding to the benzylic protons showed a strong NOE with the *ortho* protons in the first benzene ring of the BPT group, but no NOE with the alkyl chain of the imidazole, attesting that the benzylic group is pointing away from the alkyl chain.

On the basis of considerations of the molecular modeling studies carried out on some of the structures in our series, it was thought that improvement in angiotensin antagonism could be brought about by attachment of a polar group to the nitrogen of the pyridinyl or diazinyl moiety in compounds **3**–**6**. To this end the *N*-oxide derivatives were prepared. A series of *N*-imidazoyl BPT derivatives (**19**–**22**) containing the 4-diazine or the 4-pyridine ring were treated with *m*-chloroperbenzoic acid to yield the corresponding *N*-oxides **24**–**27** (Schemes 2 and 3). Detritylation of the BPT tail group in the intermediates **21**–**24** was carried out as previously described for the series of free base compounds to give the final products **28**–**31** (Tables 4 and 5). In the case of some substituted diazinylimidazole compounds (Scheme 2) such as **19b**, treatment

Table 1. 4-Diazinylimidazole Compounds

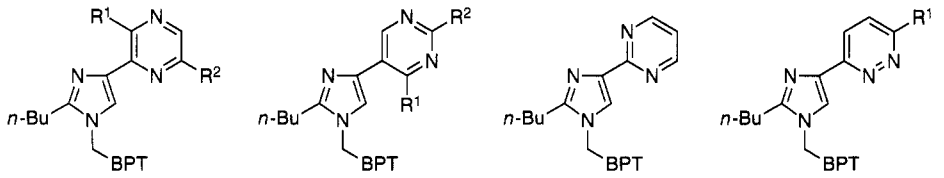

3 **4a,b** **4c** **5**

compd	R^1	R^2	mp, °C	formula[a]	binding K_i (nM)[b]
3a	H	H	117–120	$C_{25}H_{24}N_8$	40 ± 10
3b	Me	Me	118–121	$C_{27}H_{28}N_8$	7.7 ± 1.4
3c	CO_2Me	H	121–123	$C_{27}H_{26}N_8O_2$	90 ± 11
4a	H	H	117–118	$C_{25}H_{24}N_8$	42 ± 11
4b	Me	CO_2Me	125–126	$C_{28}H_{28}N_8O_2$	70 ± 6
4c	H	H	141–144	$C_{25}H_{24}N_8$	59 ± 12
5a	Me	H	196–199	$C_{26}N_{26}N_8$	12 ± 1
5b	CO_2Me	H	185–188	$C_{27}H_{26}N_8O_2$	8.8 ± 0.72

[a] Satisfactory C, H, and N elemental analyses (±0.4%) were obtained. [b] K_i for inhibition of specific binding of [^{3}H]A II to rat adrenal cortex membranes. Mean values ± sem, $n = 2–3$.

Table 2. 4-Pyridinylimidazole Compounds

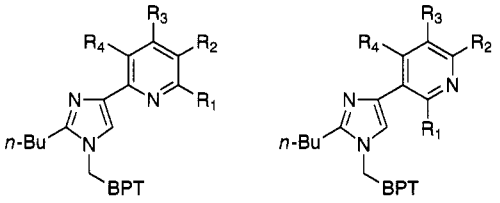

6 **7**

compd	R_1	R_2	R_3	R_4	mp, °C	formula[a]	binding K_i (nM)[b]
6a	H	H	H	CO_2Me	110–114	$C_{28}H_{27}N_7O_2$[c]	40 ± 5
6b	Me	H	H	CO_2Me	145–150	$C_{29}H_{29}N_7O_2$[c]	32 ± 5
6c	H	CO_2Me	H	H	120–123	$C_{28}H_{27}N_7O_2$	12 ± 1
6d	Me	H	Me	CO_2Me	121–124	$C_{30}H_{31}N_7O_2$	53 ± 5
6e	CO_2Me	H	H	H	201–203	$C_{28}H_{27}N_7O_2$[c]	19 ± 2
6f	Me	H	CO_2Me	H	198–201	$C_{29}H_{29}N_7O_2$[d]	1664 ± 290
6g	H	H	H	OMe	165–167	$C_{27}H_{27}N_7O$[e]	290 ± 51
6h	Me	H	H	OMe	178–181	$C_{28}H_{29}N_7O$[e]	250 ± 24
6i	OMe	H	H	H	141–147	$C_{27}H_{27}N_7O$[e,f]	25 ± 3
7a	CO_2Me	H	H	H	201–203	$C_{28}H_{27}N_7O_2$	45 ± 4
7b	H	H	CO_2Me	H	183–186	$C_{28}H_{27}N_7O_2$[c]	30 ± 7
7c	H	H	H	CO_2Me	109–111	$C_{28}H_{27}N_7O_2$	67 ± 8

[a] Satisfactory C, H, and N elemental analyses (±0.4%) were obtained, except as noted. [b] K_i for inhibition of specific binding of [^{3}H]A II to rat adrenal cortex membranes. Mean values ± sem, $n = 2–3$. [c] Compound chosen for 2D-NMR NOESY experiments. [d] N: calcd, 19.32; found, 19.82. [e] N: calcd, 20.45; found, 20.02. [f] C: calcd, 69.64; found, 68.68.

with MCPBA yielded a 1:1 regioisomeric mixture of the 1-pyrazine *N*-oxide **24b(i)** and the 4-pyrazine *N*-oxide **24b(ii)**. This mixture of regioisomers was then taken onto the final step where detritylation in refluxing methanol followed by chromatography yielded the final the 1-pyrazine *N*-oxide **28b(i)** and the 4-pyrazine *N*-oxide **28b(ii)** as separate compounds (Table 4).

Binding Affinity to the A II Receptor Site and Oral Activity of the Free Base Compounds. The series of compounds, shown in Tables 1–2, were first measured for their interaction with the receptor by way of their inhibition of [^{3}H]A II binding to rat adrenal cortex membrane preparations (AT_1 receptors). Those compounds which showed the highest potency *in vitro* in their binding assay (with K_i values of < 20 nM) were then further evaluated *in vivo* for their oral activity (Table 3) by measurement of the inhibition of the A II pressor response over a period of time (4 h), so also determining the effective duration of the A II antagonistic effect as indicated by their final calculated AUC (area under the curve) values. All the compounds tested for oral activity were employed in a dosage of 2 μmol kg^{-1}.

In our first series of compounds containing diazinyl rings attached to the imidazole (**3–5**), the results of the A II receptor binding affinities are shown in Table 1. In the series of pyrazines the absence of any substituents results in a relatively low binding affinity (**3a**), which is further decreased in the presence of electron-withdrawing groups (**3c**). The product showing the best activity was found to be that containing electron-donating substituents (**3b**) whose K_i value was 7.7 nM, which is slightly lower than that of losartan. The series of pyrimidines **4** were found to be of minor interest. In the pyridazine series of compounds, attachment of either electron-donating or electron-withdrawing substituents does not appear to influence their receptor binding affinities (K_i **5a** ≤ K_i **5b**).

From the preliminary results of these imidazole compounds bearing the π-electron deficient diazine ring in the 4-position of the imidazole ring, the effect of these groups in obtaining high binding affinities as compared

Scheme 2

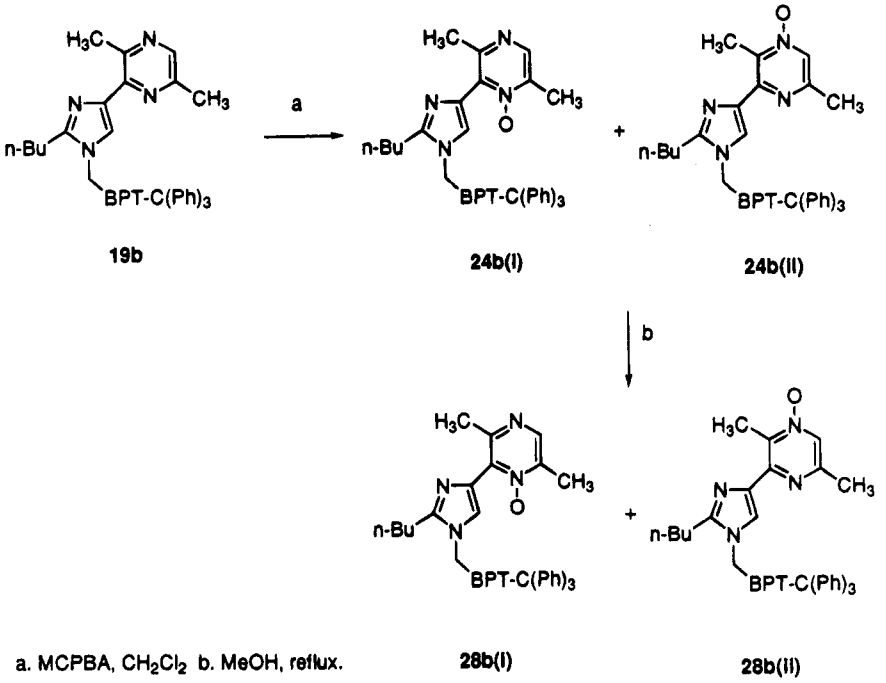

Scheme 3

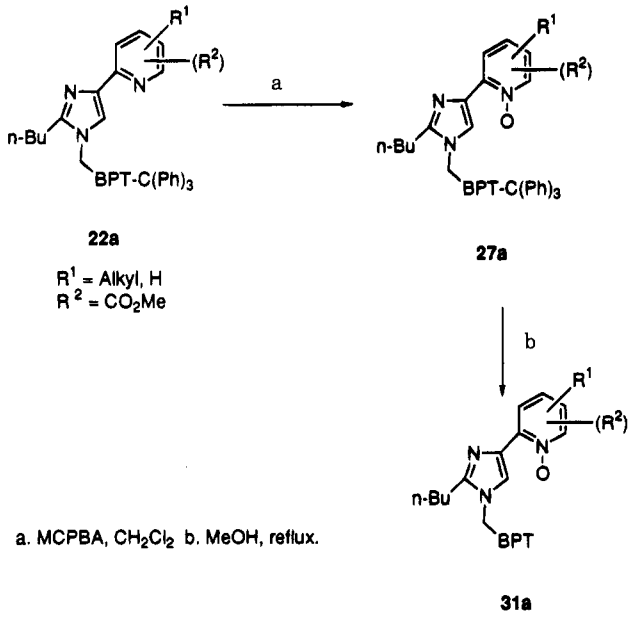

Table 3. Oral Activities of the free base 4-Diazinyl- and Pyridinylimidazole Compounds

compound	formula	max. % inhibition of AII pressor response (at time, min)[a,b]	AUC[c]
3b	$C_{27}H_{28}N_8$	−18 ± 5.7 (30)	−1365
5a	$C_{26}H_{26}N_8$	−30 ± 4.4 (15)	−2443
5b	$C_{27}H_{26}N_8O_2$	−9.3 ± 3.4 (30)	−705
6c	$C_{28}H_{27}N_7O_2$	−33 ± 8.5 (30)	−3024
6e	$C_{28}H_{27}N_7O_2$	−23 ± 2.9 (30)	−1262
6i	$C_{27}H_{27}N_7O$	−11 ± 6.3 (15)	−342
losartan		−33 ± 5.0 (210)	−3362

[a] Dosage employed was 2 μmol kg^{-1}. [b] Mean values ± sem, n = 6. [c] Area under the curve. Values (% inhibition·minutes) measured 4 h after administration.

to the halogen atom in the same position in Dupont's series of compounds, is not as great unless additional substituents are attached to the diazine ring itself.

Three of the compounds in the diazine series which showed a good binding affinity to the A II receptor, namely **3b** and the pyridazinylimidazole compounds **5a** and **5b**, were further screened for their oral activities (Table 3), with the compound **5a** showing the best activity in terms of the extent of inhibition to the pressor response (30% inhibition) and duration of action (AUC = −2443).

The second series of compounds containing the pyridinyl substituent, compounds **6a−i** and **7a−c**, the class of molecules that was the most studied, have their results for binding activity presented in Table 2. In this series, two subclasses were studied, the first group of compounds (**6a−i**) have the imidazole attached to the 2-position of the pyridine ring, and in the second group of compounds (**7a−b**), the imidazole ring is attached to the 3-position of the pyridine ring.

In the pyridinyl compounds **6** and **7** the most marked differences in the binding affinities to the receptor can be seen. The attachment of an ester substituent to the pyridine ring was first examined with the premise that the carboxylate group may interact with the receptor. This showed that the best position of this group is in position R_2 with respect to the pyridine nitrogen (K_i **6c** < K_i **6e** < K_i **6a**). Further substitution with a methyl group in **6b** brings about an increase in binding affinity to the receptor (K_i **6b** < K_i **6a**) while the introduction of a second methyl group causes a loss in activity (**6d** vs **6b**). The attachment of solely electron-donating groups to the pyridine rings like the methoxy group brings about a decrease in binding affinity with respect to those compounds containing electron-withdrawing groups (**6g** and **6h** vs **6a** and **6b**), and only in one case was a good K_i value observed (compound **6i**).

In the series of compounds **7a−c** in which the pyridine nitrogen is transposed by one ring methine from the bond linking the pyridine to the imidazole, the best position of the ester group for binding to the receptor is that of R_3 with respect to the pyridine ring nitrogen (K_i **7b** < K_i **7a** < K_i **7c**). Overall both subclasses bearing

an ester group attached to the pyridine ring have similar binding affinity.

From this second series the compounds, **6c**, **6e**, and **6i** were examined for their oral activity (Table 3). The compounds bearing an ester substituent showed the greatest inhibition to the A II pressor response, with **6c** giving the highest maximum % inhibition (33%) and longest duration of action (AUC = −3024).

The results from screening of the molecules for binding to the AT_1 receptor that have been discussed above were in turn further rationalized together with a display of these structures by the use of computer chemistry.

Molecular Modeling

The purpose of studying this series of compounds by molecular modeling was to verify the importance of substitution in the 4- or 5-position of the imidazole ring. From the structure of losartan, it was shown that the 4-position allowed for lipophilic substituents which are in addition electron withdrawing, while the 5-position of the imidazole ring required groups that were capable of interacting with the receptor by means of a hydrogen bond.[22] The introduction of electron-deficient heterocycles such as diazines and pyridines in our molecules was able to satisfy the following requirements of (a) being lipophilic and electron-withdrawing and (b) containing a heteroatom which could form a hydrogen bond with the receptor, so bringing about optimal binding affinity to the receptor. To verify this we undertook computational studies on some 4-pyridinylimidazole compounds with either electron-withdrawing or electron-donating substituents attached to the pyridine ring and to see how the electronic charge on the ring could modulate the basicity and hence the ability of the pyridine ring nitrogen to form a hydrogen bond with the receptor site. Moreover, in the modeling study we verified which would be the best position of the pyridine ring nitrogen with respect to the bond linking the ring to the imidazole to have the maximum receptor interaction.

To correlate the results of the binding data for our compounds with their structure, we chose to examine the molecular electrostatic potential (MEP)[23] of some of the molecules in the series, as an index for recognition and as a tool to evaluate the interaction energy.

The MEP is a measurable quantity that depends on the geometry and charge distribution of the molecule. Its value in a point outside the molecule coincides with the interaction energy between the molecule and a bare proton located at that point. It is therefore a very good index of the capability of a molecule to establish polar and nonpolar interactions with its molecular environment. In all cases where the receptor site geometry is unknown, descrimination between several structures as possible drug candidates is greatly aided by the examination of the structure and corresponding MEP of molecules which bind to the receptor. The common features of the MEP are thus, highlighted, and on the basis of the presence or extent of these features, it is possible by inference to choose from several structures which ones may be more active than the others.

In order to determine reliable structures for the systems examined, their flexibility, which is limited due to presence of aromatic rings, was studied by *ab initio*

Scheme 4

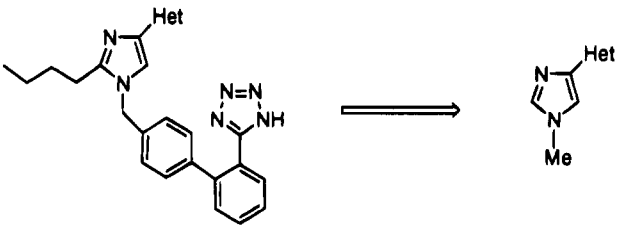

calculations[24] being carried out on model systems (Scheme 4) in which the *n*-butyl chain is replaced by a hydrogen atom and the methylbiphenylyltetrazole is replaced by a methyl group. This general model structure was chosen to limit the number of atoms contained in these compounds and so allow these calculations to be carried out at the SCF level, making use of the 3-21G basis set. The conformational degrees of freedom were scanned in the flexible rotor approximation. In addition, two different conformers of one of the compounds were studied at the 6-31G* level in order to check the quality of the 3-21G description.

In order to evaluate the importance of substituents attached to the heterocycle, we introduced onto the ring alternately and in various positions electron-withdrawing groups (CO_2Me, NO_2, CN) and electron-donating groups (OMe, CH_2OAc, $OCOCH_3$). The geometry optimization had shown that, *in vacuo*, the molecules tend to arrange themselves into an orientation in which the nitrogen of the heterocycle (that is of the pyridine) is furthest away from the nitrogen in the 3-position of the imidazole ring (i.e., an *anti* arrangement) as a result of strong forces of repulsion between the two negative potential zones situated around the two nitrogens owing to the presence of two electron lone pairs (Figure 3). In this orientation the lone pair of the pyridine nitrogen occupies the space vicinal to the hydrogen in position 5 of the imidazole ring. This spatial arrangement in our molecules would exclude the possibility that the carboxyl group attached to the pyridine or diazine ring could interact with the receptor by means of a hydrogen bond as the hydroxymethyl group of losartan. Therefore, in our structures the carboxyl group acts only as an electron-withdrawing group.

Despite the large electrostatic effect produced in the *syn* arrangement caused by the facing of the two N atom lone pairs, this orientation of the two aromatic rings could be favored in a polar solvent.[25] It also turned out that these structures having the *syn* arrangement *in vacuo* are destabilized by just 0.2−7.6 kcal/mol with respect to their conformation having the *anti* arrangement.

This spatial arrangement in these molecules was also confirmed by the NMR data which indicated that also in solution this *anti* arrangement between the imidazole

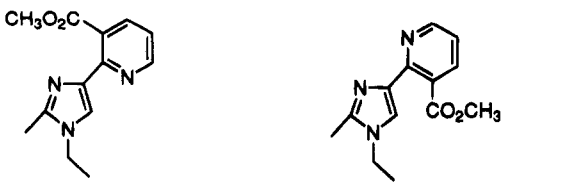

anti-arrangement (favored) *syn*-arrangement (disfavored)

Figure 3.

and pyridine nitrogen is preferred. For example, compound **6a**, bearing the ester group *ortho* to the bond linking the imidazole, in its 2D NOESY spectrum showed no cross peak between the ring position 5 imidazole proton and the methyl of the ester group. It should be pointed out that although the NMR studies are indicative of the conformation of these molecules in solution, this may still not reflect their conformation when bound to the Angiotensin receptor. Furthermore, even though the calculations on the geometry of these molecules were carried out *in vacuo*, it is expected that these structures would also reflect more closely the geometries of the molecules bound inside the receptor site than the same unbound molecules in solution due to the generally hydrophobic nature of receptor sites.[26]

An exception to the NMR data, however, was found in the case of molecules bearing a methoxy group joined to the pyridine ring. Although according to the calculations these molecules prefer to take up the *anti* arrangement *in vacuo*, corresponding to the structure seen in Figure 3, the NMR studies in solution of **6g**, which bears the methoxy group vicinal to the pyridine ring nitrogen, revealed in its NOESY spectrum a strong cross peak between the imidazole proton in ring position 5 and the methoxy group, indicating rather than the following *syn* arrangement shown below (Figure 4) is favored.

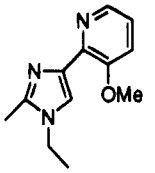

Figure 4.

The calculation on the model of compound **6g** was checked further by repeating the geometry optimization and MEP using the higher basis set 6-31G*. At the initial 3-21G level, the energy difference of 2.44 kcal/mol in favor of the *anti* arrangement of the two ring nitrogens was found. The given description of the two basis sets for both conformers is analogous both from the view point of geometry and electronics. The difference in energy between the two conformers of the model of **6g** was found to decrease to 2.01 kcal/mol, going to the 6-31G* level with a torsion angle between the two rings for the *anti*-conformer being 4° higher compared to the same structure at the 3-21G level. All the other variations in the torsion angles between the two basis sets are of the order of 1° or less. Also the electrostatic potential maps and the V_{min} value do not sustain any appreciable variations on going from the 3-21G to the 6-31G* basis set.

The MEP of a few model systems related to our series of compounds were examined (Figure 5). It was possible to single out two common features of the MEPs of these pharmacologically most active compounds compared to the less active compounds in our series, namely (i) the almost perfect coplanarity of the two linked heteroaromatic rings even when the N atoms are either in the *syn* or the *anti* position and (ii) the presence of sharply negative lobes in the MEP, close to the diazine or pyridine ring nitrogen and that of the position-1 imidazole ring nitrogen. The more negative this zone is, the more active the compound.

It was clear at this point that the following conclusions regarding the relationship between structure and activity of our molecules were able to be drawn. Firstly, to maximize the negative potential that includes the part of space between the N-1 imidazole nitrogen and the pyridine or diazine ring nitrogen, it is necessary that the latter N atom in both cases be ortho with respect to the bond to the imidazole ring itself. An electron-donating group (e.g., methyl) being attached to the position vicinal to the pyridine or diazine nitrogen increases the basicity of that nitrogen and consequently the negative zone around it. Secondly, it is necessary to maintain a large degree of coplanarity between the two heterocyclic moieties.

These common features, inferred from MEP studies of the free base compounds to rationalize their activity, made us suppose that an enlargement of the negative zone (an index of possible interaction with the receptor by hydrogen bonding) by derivitization of the pyridine or diazine ring nitrogen as its *N*-oxide could favor an increased binding affinity of this class of molecules with the receptor. Thus the MEP values of the model systems of our most important compounds as their *N*-oxide derivatives were calculated to see if this hypothesis held true. To explain the results, the MEP of compounds **3b** (K_i = 77 nM), **6b** (K_i = 32 nM), and **6c** (K_i = 12 nM) were chosen (Figure 6) and compared with the MEP of their *N*-oxide derivatives (Figure 7). It was found that attachment of an oxygen to the pyridine or diazine ring nitrogen in the model structures of **3b**, **6b**, and **6c** causes a marked increase in the size of the zone of negative potential around these nitrogen atoms. These negative regions (as also in the case of the free base compounds **3b** and **6c**) presented an outward channel, with a wide solid angle which in some cases was close to 180°.

At this point the data obtained from the screening of our compounds for binding could be rationalized on the basis of an expansion of the negative potential between the pyridine and imidazole nitrogens and on the coplanarity between the two rings. The introduction in the molecular modeling calculations of the *N*-oxide group into our structures brought about an increase in the negative potential between the two nitrogens, leading us to suppose that for these compounds there would be a greater affinity to the receptor. The validity of this hypothesis, in the search for a more active compound in this class of molecules, was subsequently tested out by preparing and screening the *N*-oxide derivatives of some of the compounds in this series.

Binding Affinity to the A II Receptor Site and Oral Activities of the *N*-Oxide Derivatives. On the basis of the molecular modeling studies discussed above, we then drew our attention to studying the *in vitro* and *in vivo* activities of the *N*-oxide derivatives of the 4-diazinyl- and of the 4-pyridinylimidazoles as a way to increase binding affinities by attachment of this polar group to the ring nitrogen of the diazine/pyridine which could interact better with the pocket of the A II receptor site than the free base itself.

As the molecular modeling calculations are carried out on molecules *in vacuo* and the pharmacological studies on compounds in aqueous solution, it was also necessary to prepare the *N*-oxide derivatives of those

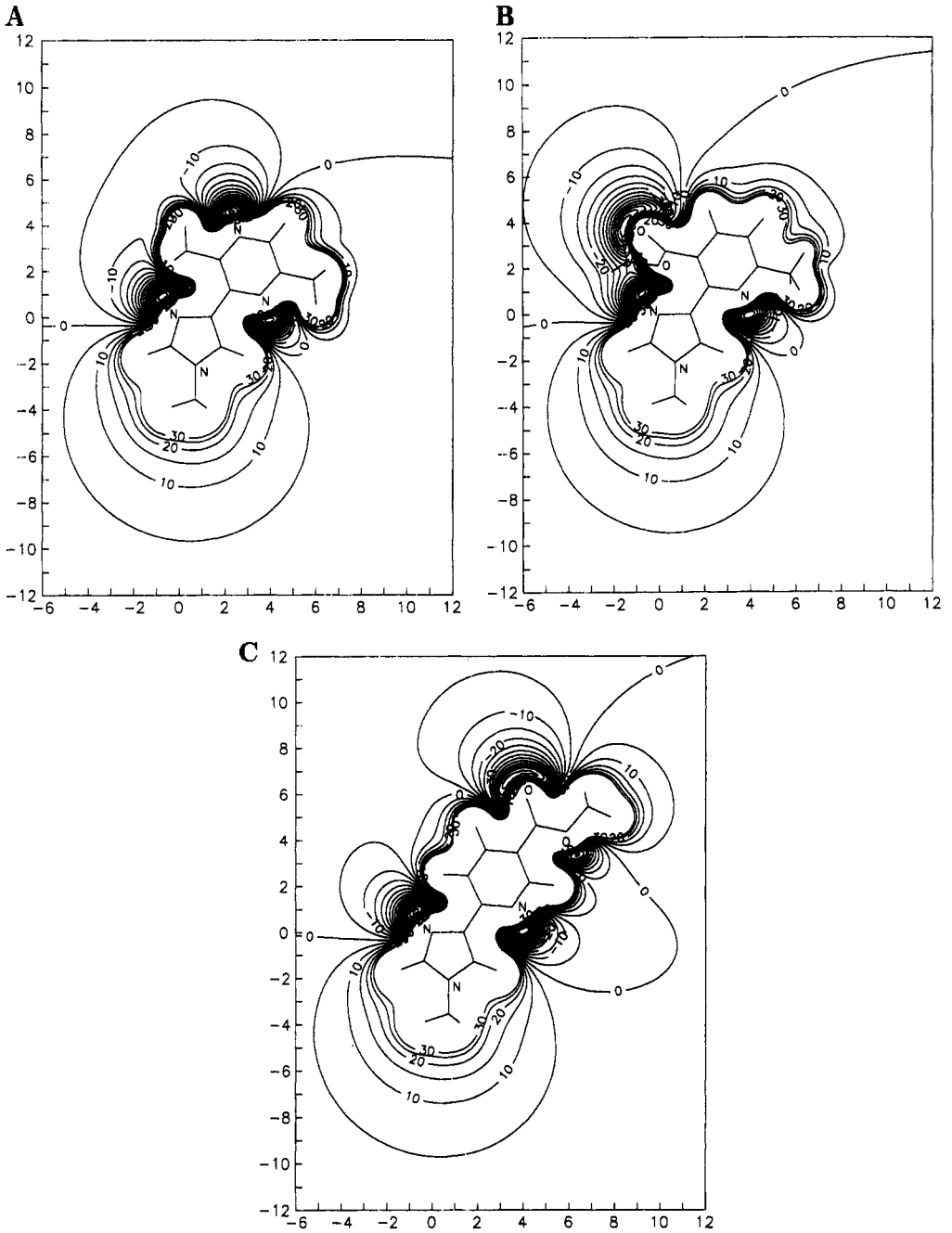

Figure 5. Molecular electrostatic maps for (A) **3b**, (B) **6b**, and (C) **6c** in the molecular plane (coordinates in angstroms, isopotential lines spaced by 5 kcal/mol, MEP calculations at the 3-21G/SCF level on geometries using the 3-21 G basis set).

compounds not having the structural requirements which indicate an improved binding. This was in order to have a comparison which would help confirm the hypothesis resulting from the MEP data on those model systems which did point to improved activity on going from the free base to the *N*-oxide.

The results for the *N*-oxide derivatives of the 4-diazinylimidazolyl compounds **28–30** are shown in Table 4. As predicted from molecular modeling, only those compounds which had the required structural features showed an increased activity (**28b(i)** and **28b(ii)**), while the others remained unchanged (**29a** and **29b**) or even showed a lower activity (**28a**, **30a**, and **30b**) compared to their free bases.

Of the diazine *N*-oxide derivatives examined for oral activity (Table 6), the regioisomers 3,6-dimethylpyrazine *N*-oxides **28b(i)** and **28b(ii)** revealed for the 1-*N*-oxide **28b(i)** an elevated inhibition of the A II pressor response (43% inhibition) together with a higher effective duration of the antagonist effect (AUC = −6690) compared to its free base compound **3b** (AUC = −1365). The pyrazine *N*-oxide derivatives **30a(i)** and **30a(ii)** showed a similar percentage of inhibition to the A II pressor compared to their free base precursor **5a**, but in the case of the 1-*N*-oxide isomer **30a(i)**, bearing the stabilizing methyl group vicinal to the N−O, the duration of the effect increased compared to the free base (AUC **30a(i)** = −4731 vs AUC **5a** = −2443).

With the pyridine *N*-oxide derivatives **31** (Table 5), improved binding affinities of the resulting *N*-oxide derivatives with respect to their free bases were observed in compounds where an electron-donating group was positioned ortho or para to the pyridine ring nitrogen, as predicted by molecular modeling. Thus the *N*-oxide compound **31b** (K_i = 4.5 nM) showed a 7-fold increase in activity compared to the parent free base

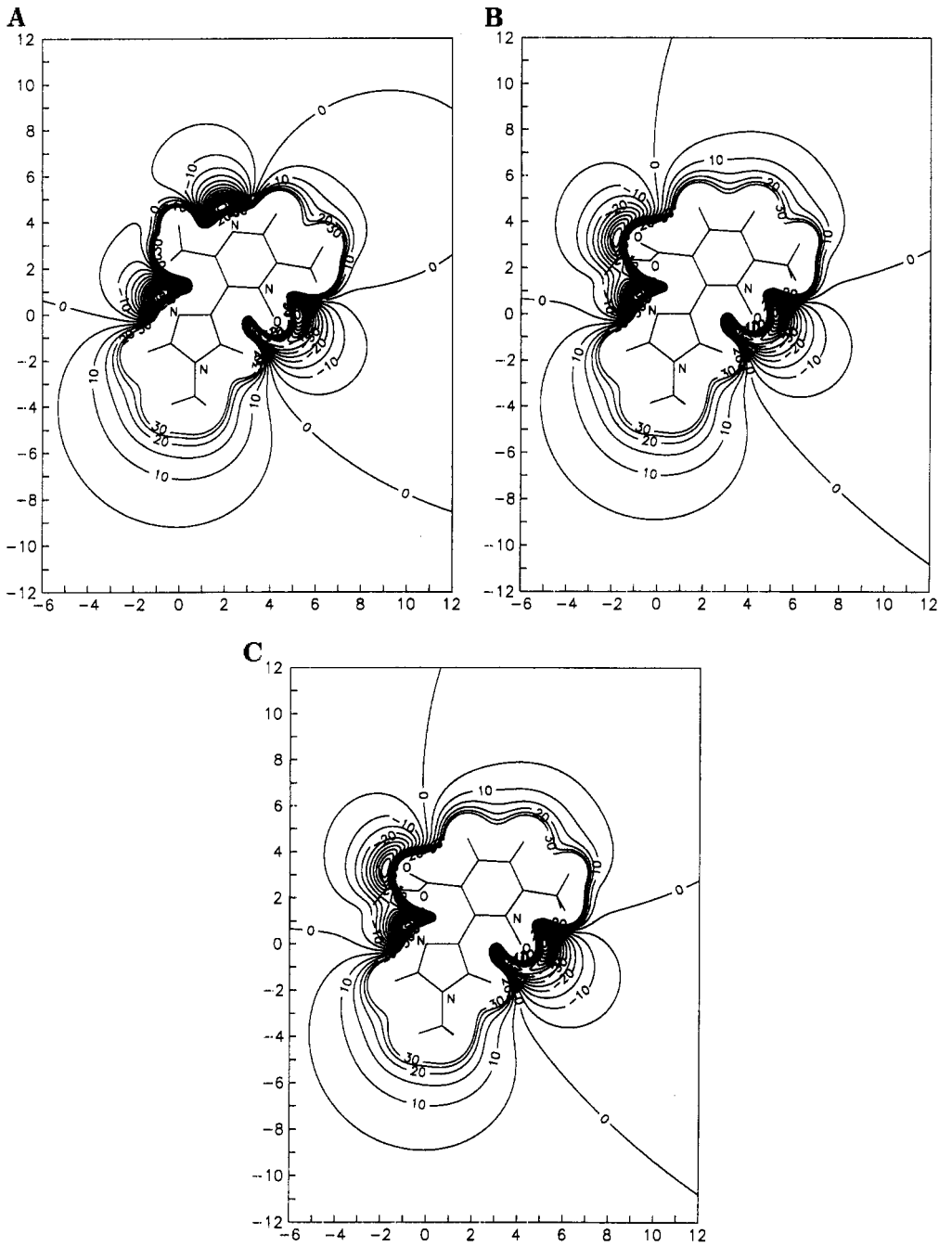

Figure 6. Molecular electrostatic maps for the *N*-oxide derivatives of (A) **3b**, (B) **6b**, and (C) **6b** in the molecular plane (coordinates in angstroms, isopotential lines spaced by 5 kcal/mol, MEP calculations at the 3-21G/SCF level on geometries using the 3-21 G basis set).

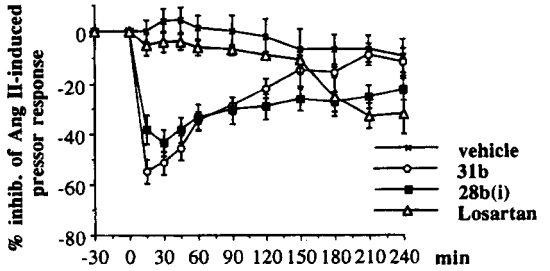

Figure 7. Effect of orally administered vehicle and 2 μmol kg^{-1} of compound **28b(i)**, **31b** or losartan on the angiotensin II-induced pressor response in conscious normotensive rats. Values represent the mean ± sem, $n = 6$.

6b (K_i = 32 nM) as also did compound **31c** (K_i = 9 nM) compared to its free base **6d**, which gave a K_i value of 53 nM.

The pyridine *N*-oxide compounds **31b**, **31c**, and **31f** were screened for oral activity (Table 6) with **31b** showing the best oral activity with 55% inhibition of the A II pressor response together with a long duration of the effect (AUC = −5912). Again stabilization of the *N*-oxide group by attachment of an electron-donating methyl group adjacent to the ring nitrogen contributes to an enhanced activity *in vivo*. The peak inhibition of A II-induced pressor response obtained both with free base and the *N*-oxide derivatives (Figure 7) occurred within 15−30 min and then decreased, indicating a rapid onset of the effect. Conversely, in the case of the reference compound losartan, a slow onset of the effect was observed (peak effect = 210 min). The reason for this difference may be ascribed mainly to the progressive hepatic conversion of losartan to the more active compound EXP 3174.[27]

Table 4. 4-Diazinyl *N*-Oxide Imidazole Compounds

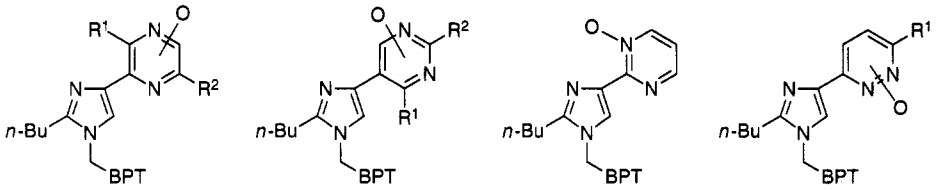

compd	R^1	R^2	*N*-oxide isomer	mp, °C	formula[a]	binding K_i (nM)[b]
28a	H	H	1-*N*-oxide	nd[c]	$C_{25}H_{24}N_8O$	243 ± 73
28b(i)	Me	Me	1-*N*-oxide	109–113	$C_{27}H_{28}N_8O$[d]	2.5 ± 0.49
28b(ii)	Me	Me	4-*N*-oxide	208–212	$C_{27}H_{28}N_8O$	4.4 ± 0.42
29a	H	H		112	$C_{25}H_{24}N_8O$	25 ± 2
29b	H	H		237–243	$C_{25}H_{24}N_8O$	61 ± 7
30a(i)	Me	H	1-*N*-oxide	227–229	$C_{26}H_{26}N_8O$	44 ± 1
30a(ii)	Me	H	2-*N*-oxide	133–135	$C_{26}H_{26}N_8O$	40 ± 13
30b	CO_2Me	H	2-*N*-oxide	145–149	$C_{27}H_{26}N_8O_3$	54 ± 5

[a] Satisfactory C, H, and N elemental analyses (±0.4%) were obtained. [b] K_i for inhibition of specific binding of [^{3}H]A II to rat adrenal cortex membranes. Mean values ± sem, n = 2–3. [c] Compound was a resinous solid which failed to give an accurate melting point. [d] Compound chosen for 2D-NMR NOESY experiments.

Table 5. 4-Pyridinyl *N*-Oxide Imidazole Compounds

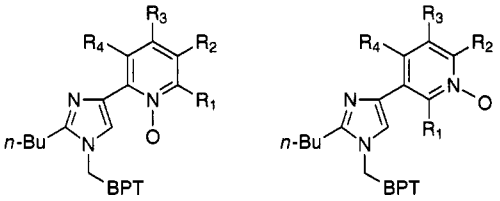

compd	R_1	R_2	R_3	R_4	mp, °C	formula[a]	binding K_i (nM)[b]
31a	H	H	H	CO_2Me	215–218	$C_{28}H_{27}N_7O_3$	29 ± 2
31b	Me	H	H	CO_2Me	200–204	$C_{29}H_{29}N_7O_3$[c]	4.5 ± 1.1
31c	Me	H	Me	CO_2Me	219–223	$C_{30}H_{31}N_7O_3$	9.1 ± 2.1
31d	H	CO_2Me	H	H	218–221	$C_{28}H_{27}N_7O_3$	27 ± 4
31e	Me	H	CO_2Me	H	198–201	$C_{29}H_{29}N_7O_2$	180 ± 53
31f	Me	H	H	OMe	138–142	$C_{28}H_{29}N_7O_2$[c]	38 ± 8
32	H	H	CO_2Me	H	127–132	$C_{28}H_{27}N_7O_3$[c]	41 ± 8

[a] Satisfactory C, H, and N elemental analyses (±0.4%) were obtained. [b] K_i for inhibition of specific binding of [^{3}H]A II to rat adrenal cortex membranes. Mean values ± sem, n = 2–3. [c] Compound chosen for 2D-NMR NOESY experiments.

Table 6. Oral Activities of the *N*-Oxide Derivatives of 4-Diazinyl- and Pyridinylimidazole Compounds

compound	formula	max % inhibition of AII pressor response (at time, min)[a,b]	AUC[c]
28b(i)	$C_{27}H_{28}N_8O$	−44 ± 5.6 (30)	−6690
28b(ii)	$C_{27}H_{28}N_8O$	−21 ± 8.6 (15)	−2725
30a(i)	$C_{26}H_{26}N_8O$	−35 ± 3.4 (15)	−4731
30a(ii)	$C_{26}H_{26}N_8O$	−27 ± 9.2 (15)	−2672
31b	$C_{29}H_{29}N_7O_3$	−55 ± 4.8 (15)	−5912
31c	$C_{30}H_{31}N_7O_3$	−29 ± 8.0 (15)	−4515
31f	$C_{28}H_{29}N_7O_2$	−22 ± 6.4 (30)	−2583
losartan		−33 ± 5.0 (210)	−3362

[a] Dosage employed was 2 μmol kg^{-1}. [b] Mean values ± sem, n = 6. [c] Area under the curve. Values (% inhibition·minutes) measured 4 h after administration.

Overall, comparing both series of compounds, in the case of the diazine *N*-oxides, where the *N*-oxide group is stabilized by electron-donating groups adjacent to the ring nitrogen, binding affinity is slightly improved with respect to the free bases, whereas in the series of pyridine *N*-oxides containing electron-donating groups next to the pyridine ring nitrogen, there is a marked increase in the binding with respect to their free bases as well as improved oral activity, thus verifying the interesting activity which we had presumed on the basis of our computational studies of these molecules.

Conclusion

A new class of antagonists of angiotensin II for the AT_1 receptor have been identified and have as their main characteristic the absence of any substituents in position 5 of the imidazole ring as in losartan. The substitution of the chlorine atom in position 4 of the imidazole ring with an electron-deficient heterocyclic group bearing a heteroatom such as nitrogen in an appropriate part of the space results in molecules with activities in the nanomolar range.

On the basis of the hypothesis resulting from the molecular modeling studies, the introduction of the *N*-oxide group was found to increase the interaction of these compounds with the receptor as well as to give improved *in vivo* oral activity. This underlies the predictive value of the MEP mapping technique applied to these molecules. Some of the compounds in the series such as **28b(i)** and **31b** have been selected for further in depth studies.

Experimental Section

Melting points are uncorrected and were measured with a Reichert-Thermovar hot-stage melting point apparatus. Elemental analyses were performed by Microan. Lab. of Instituto Chimica Farmaceutica Università di Pisa. Analytical results are indicated by the element symbols and are within ±0.4%. Column chromatography was performed with E. Merck silica gel 60 (230–400 mesh). ^{1}H NMR (200 MHz) spectra were measured with a Bruker 200 AC spectrometer. Chemical shifts are expressed in PPM (δ) downfield from TMS as an internal standard. Coupling constants are given in hertz. NMR 2D NOESY experiments were carried out with ca. 0.2 M solutions of the chosen compound, degassed by freeze–pump–thaw cycles. NOESY experiments for compounds **6a**, **6b**, and **31f** were carried out in d_6-DMSO, for **6g** in d_6-DMSO/$CDCl_3$ (1:1), for **6i** in d_6-DMSO/CD_3OD (1:1), for **6e**, **31b**, and **32** in $CDCl_3$, for **28b(i)** in $CDCl_3$/CD_3OD (1:1), and for **7b** in $(CD_3)_2CO$. The 2D NOESY were recorded in phase sensitive mode with the sequence RD-90-t_1-90-t_M-90-AQ. A mixing time of 1 s was used. The pulse delay was maintained at 6 s. The data sizes were 256w in F1 and 1K in F2 and the data were zero filled in F1 before Fourier transformation to yield a 1K × 1K data matrix. The data were processed using a gaussian function in both dimensions.

Molecular Modeling Computational Details. The *ab initio* calculations at the SCF level making use of the 3-21 G and 6-31 G* basis sets were carried using *Gaussian* 92 at ICQEM.[24] The conformational degrees of freedom were scanned in the flexible rotor approximation. The molecular electrostatic maps were drawn with SURFER.[28]

2-Butyl-1-[[2-(trimethylsilyl)ethoxy]methyl]-1*H*-imidazole (9). 1-[[2-(Trimethylsilyl)ethoxy]methyl]-1*H*-imidazole,[29] **8** (27.04 g, 0.14 mol), was combined with TMEDA (15.9 g, 0.14 mol) in THF (690 mL). The solution was cooled to −40 °C, and *n*-butyllithium (89 mL, 1.6 M, 0.14 mol) was added dropwise via syringe, resulting in a fawn-colored solution. After the mixture was stirred fo 30 min, *n*-butyl iodide (21 mL, 0.15 mol) was added and the reaction left to stir overnight with gradual warming up to room temperature. The reaction was quenched with water (580 mL) and the aqueous phase separated and extracted with chloroform (3 × 580 mL). The combined organic fractions were washed with aqueous sodium thiosulfate solution (2 × 580 mL) and water (580 mL), followed by drying ($MgSO_4$). Removal of solvent under reduced pressure and purification of the crude material by flash chromatography (EtOAc:petroleum ether, 80:20) gave 27.68 g (80%) of **9** as a yellow oil: ^{1}H NMR ($CDCl_3$) 0.03 (9H, $SiMe_3$), 0.88–1.01 (3H, 2H, CH_3 and CH_2SiMe_3), 1.42 (2H, sext, J = 5.2), 1.79 (2H, quint, J = 4.63), 2.75 (2H, t, J = 8.1), 3.50 (2H, t, J = 5.3), 5.23 (2H, s), 6.93 (1H, d, J = 1.3), 6.97 (1H, d, J = 1.3).

2-Butyl-1-[[2-(trimethylsilyl)ethoxy]methyl]-5-(tributylstannyl)-1*H*-imidazole (10). Compound **9** (3.96 g, 15.6 mol) was dissolved in ether (100 mL), and *n*-butyllithium (6.24 mL, 2.50 M, 15.6 mmol) was added via syringe at room temperature. The lithiated imidazole precipitated out, and the suspension was stirred for 1 h. After this time, tri-*n*-butylstannyl chloride (4.42 mL, 16.3 mmol) was added. The resulting yellow solution was then left to stir overnight. The reaction was quenched by addition of saturated NH_4Cl solution (100 mL) followed by ether (100 mL). The two layers were separated, and the ether layer was further washed with brine (100 mL). Drying of the extract (Na_2SO_4) and removal of solvent under reduced pressure gave 9.02 g of crude product whose titre was analyzed by ^{1}H NMR. The titre was between 60 and 80% with respect to **10**. The crude material was used without further purification in the next step: ^{1}H NMR ($CDCl_3$) −0.0032 (9H, s, $SiMe_3$), 0.85–1.52 (27H, 3H, and 2H, $SnBu_3$, CH_2SiMe_3, and CH_3), 2.7 (2H, t, J = 8.0), 3.41 (2H, t, J = 8.7), 5.1 (2H, s), 6.92 (1H, s).

2-Butyl-5-(3,6-dimethylpyrazin-2-yl)-1*H*-imidazole (15b). Steps 4 and 5. The stannylimidazole **10** (6 g, 80% titre, 8.8 mmol) was dissolved in dry dioxan (85 mL), and 3,6-dimethyl-2-chloropyrazine (1.51 g, 10.6 mmol) was added together with 2,6-di-*tert*-butyl-4-methylphenol (ca. 5 mg) and tetrakis(triphenylphosphine)palladium(0) (0.5 g, 0.45 mmol). After the reaction mixture was refluxed for 3 h, ether (100 mL) and saturated NaF solution (100 mL) were added. The two phases were stirred overnight and then filtered through Celite, and the organic phase was separated. The aqueous phase was extracted with further ether (2 × 100 mL). The combined organic extracts were washed with brine (100 mL) and dried ($MgSO_4$). Removal of solvent under reduced pressure gave 6.0 g of crude coupling product which was then deprotected according to method A (step 5). The crude product obtained above (6.0 g, ca. 8.8 mmol) was combined with 5 N aqueous hydrochloric acid (30 mL) and methanol (15 mL) and the mixture refluxed for 3 h, resulting in a clear solution. The reaction mixture was then cooled and filtered through Celite and the filtrate washed with ethyl acetate (3 × 45 mL). The aqueous phase was made alkaline with 35% NaOH and then extracted with dichloromethane (5 × 30 mL). The combined organic extracts were washed wth water (30 mL) and brine (30 mL) and dried ($MgSO_4$). Purification of the crude product by flash chromatography ($CHCl_3$:MeOH, 95:5) gave 1.61 g (80%) of **15b**: mp 116–118 °C; ^{1}H NMR ($CDCl_3$) 0.99 (3H, t, J = 7.30), 1.43 (2H, sext, J = 7.7) 1.76 (2H, quint, J = 5), 2.51 (3H, s), 2.70 (3H, s), 2.81 (2H, t, J = 7.4), 7.44 (1H, s), 8.16 (1H, s), 10.17 (1H, br s).

2-Butyl-5-[6-(methoxycarbonyl)pyridazin-3-yl]-9-[[2-(trimethylsilyl)ethoxy]methyl]-1*H*-imidazole (13b). Step 4. The stannylimidazole derivative **10** (6 g, 80% titre, 8.9 mmol) was dissolved in dry dioxan, and methyl 3-chloropyridazine-6-carboxylate[16] (1.55 g, 9 mmol) was added together with 2,6-di-*tert*-butyl-4-methylphenol (5 mg) and tetrakis(triphenylphosphine)palladium(0) (0.51 g, 0.45 mmol). The reaction mixture was refluxed for 7 h, cooled, and then diluted with ether (100 mL) and saturated sodium fluoride solution (100 mL). The two phases were stirred for 3–4 h and then filtered through Celite. The organic phase was separated, washed with water (100 mL) and brine (100 mL), and finally dried (Na_2SO_4). Removal of solvent under reduced pressure and purification by flash chromatography (EtOAc) yielded 2.63 g (76%) of **13b** as a pale yellow-colored solid: R_f (EtOAc) = 0.41; ^{1}H NMR ($CDCl_3$) −0.04 (9H, $SiMe_3$), 0.87 (2H, t, J = 7.40), 0.96 (3H, t, J = 7.3), 1.40 (2H, sext, J = 7.2), 1.80 (2H, quint, J = 5.5), 2.9 (2H, t, J = 8.1), 3.5 (2H, t, J = 8.0), 4.1 (3H, s), 6.1 (2H, s), 7.57 (1H, s), 7.82 (1H, d, J = 9), 8.13 (1H, d, J = 8.9).

2-Butyl-5-[6-(methoxycarbonyl)pyridazin-3-yl]-1*H*-imidazole (17b). Step 5. Method B. A mixture of **13b** (3.66 g, 9.39 mmol) in methanol (50 mL) and 7 M methanolic HCl (20 mL, 0.141 mol) was refluxed for 4 h, resulting in a clear solution. Then sodium bicarbonate (12 g) was added portionwise and the suspension evaporated down. The resulting residue was taken up in ethyl acetate and water. The two phases were stirred magnetically, and 2 N aqueous NaOH was added until pH 10–12. The organic layer was separated and the remaining aqueous layer further extracted with ethyl acetate. The combined organic extracts were dried (Na_2SO_4), and the solvent was removed under reduced pressure. Purification by flash chromatography ($CHCl_3$:MeOH, 9:1) gave 1.51 g (62%) of **17b** as a buff-brown solid: mp 187–189 °C; ^{1}H NMR ($CDCl_3$) 0.92 (3H, t, J = 7.2), 1.44 (2H, sext, J = 7.6), 1.77 (2H, quint, J = 7.8), 2.86 (2H, t, J = 7.7), 4.1 (3H, s), 8.1 (1H, d, J = 14), 8.2 (1H, s), 8.25 (1H, d, J = 10.5), 10.7 and 11.15 (1H, br s, NH tautomers).

2-Butyl-4-(3,6-dimethylpyrazin-2-yl)-1-[[1′-[1-triphenylmethyl)-1*H*-tetrazol-5-yl][1,1′-biphenyl]-4-yl]methyl]-1*H*-imidazole (19b). Step 6. Sodium hydride (181 mg, 60% dispersion in oil, 4.52 mmol) was added to a solution of **17b** (800 mg, 3.47 mmol) in DMF (25 mL). After the mixtue was stirred for 1 h, 2.58 g of **23** (75%, 3.47 mmol) in DMF (35 mL) was added. After stirring overnight at room temperature, the mixture was poured into water and ethyl acetate. The mixture was made alkaline (pH 12) by addition of 2 N NaOH, the two phases were separated, and the aqueous phase was extracted with further ethyl acetate (3 × 60 mL). The combined organic extracts were washed with 2 N NaOH (60 mL) and dried ($MgSO_4$). Solvent was removed under reduced pressure and the crude residue purified by flash chromatography ($CHCl_3$:MeOH, 98:2). This gave 1.59 g (65%) of **19b** as an ivory solid:

mp 72–75 °C; ^{1}H NMR ($CDCl_3$) 0.91 (3H, t, J = 7.4), 1.39 (2H, sext, J = 7.7), 1.74 (2H, quint, J = 7.9), 2.52 (3H, s), 2.68 (2H, t, J = 8.10), 2.78 (3H, s), 4.99 (2H, s), 6.38–7.95 (24H, m), 8.18 (1H, s).

2-Butyl-4-[6-(methoxycarbonyl)pyridazin-3-yl]-1-[[1′-[1-(triphenylmethyl)-1*H*-tetrazol-5-yl][1,1′-biphenyl]-4-yl]methyl]-1*H*-imidazole (21b). Step 6. Sodium hydride (123 mg, 60% dispersion in oil, 3.08 mmol) was suspended in dry DMF (7 mL), and a solution of **17b** (800 mg, 3.08 mmol) in DMF (7 mL) was added dropwise. The resulting solution was stirred for 1 h, and then a solution of **23** (2.40 g, 72%, 3.09 mmol) in DMF (15 mL) was added at 0 °C. After addition was complete, the reaction mixture was left to stir overnight at room temperature. The mixture was then poured into ice/water and ethyl acetate added. The two phases were stirred together, and solid Na_2CO_3 was added to make the aqueous phase alkaline. The two phases were then separated, and the aqueous phase was extracted with further ethyl acetate (2 × 30 mL). The combined organic extracts were washed with brine and dried (Na_2SO_4), and solvent was removed under reduced pressure. Purification by flash chromatography (EtOAc:hexane, 90:10) gave 1.96 g, (86%) of **21b** as a colorless solid: mp 190–193 °C; ^{1}H NMR ($CDCl_3$) 0.91 (3H, t, J = 7.2), 1.41 (2H, sext, J = 7.6), 1.74 (2H, pent, J = 7.6), 2.70 (2H, t, J = 7.8), 4.1 (3H, s), 5.0 (2H, s), 6.85–7.83 (23H, m), 7.8 (1H, s), 8.15 (1H, d, J = 8.9), 8.23 (1H, d, J = 8.7).

2-Butyl-4-[6-(methoxycarbonyl)pyridazin-3-yl]-1-[[2′-(1*H*-tetrazol-5-yl)[1,1′-biphenyl]-4-yl]methyl]-1*H*-imidazole (5b). Step 7. Obtained from **21b** (600 mg, 0.815 mmol) being refluxed in methanol (25 mL) for 5 h. After this time the methanol was evaporated under reduced pressure and diethyl ether added to the residue causing the product to crystallize out. The solid was filtered, washed several times with ether, and finally dried by suction. This gave 400 mg (99%) of **5b** as an ivory solid: mp 185–188 °C; ^{1}H NMR ($CDCl_3$) 0.93 (3H, t, J = 7.5), 2H, sext, J = 7.6), 1.70 (2H, quint, J = 8.3), 4.0 (3H, s), 5.20 (2H, s), 7.13–7.70 (9H, m), 7.91 (1H, s), 8.14 (1H, d, J = 8.8), 8.23 (1H, d, J = 8.9). Anal. ($C_{27}H_{26}N_8O_2$) C, H, N.

2-Butyl-4-(3,6-dimethyl-*N*-oxopyrazin-2-yl)-1-[[1′-[1-(triphenylmethyl)-1*H*-tetrazol-5-yl][1,1′-biphenyl]-4-yl]methyl]-1*H*-imidazole Regioisomers 24b(i) and 24b(ii). A 1.14 g (1.61 mmol) sample of **19b**, obtained by the scheme described, was dissolved in dichloromethane (20 mL), and MCPBA (0.47 g, 65%, 1.77 mmol) in dichloromethane (30 mL) was then added dropwise at room temperature. The reaction mixture was stirred for 4 h and then washed with 0.1 N NaOH (2 × 50 mL), the organic phase was then dried ($MgSO_4$), and solvent was removed under reduced pressure to give a yellow resin of crude **24b**. Flash chromatography using dichloromethane with increasing proportions of methanol (CH_2Cl_2:MeOH, 99:1–97:3) as the eluting mixture gave 343 mg of precursor **19b**, 335 mg (28%) of the pyrazine 1-*N*-oxide regioisomer **24b(i)**, and 326 mg (28%) of a mixture of *N*-oxide regioisomers **24b(i)** and **24b(ii)**: mp °C, **24b(i)** 69–72 °C; ^{1}H NMR ($CDCl_3$) **24b (i)** 0.90 (3H, t, J = 7.2), 1.37 (2H, J = 7.4), 1.70 (2H, pent, J = 7.4), 2.45 (3H, s), 2.61 (2H, t, J = 7.2), 3.00 (3H, s), 4.99 (2H, s), 6.86–7.91 (23H, m), 8.17 (1H, s), 8.31 (1H, s).

2-Butyl-4-(3,6-dimethyl-*N*-oxopyrazin-2-yl)-1-[[2′-[1-(triphenylmethyl)-1*H*-tetrazol-5-yl][1,1′-biphenyl]-4-yl]methyl]-1*H*-imidazole [28b(i) and 28b(ii)]. A 280 mg (0.387 mmol) sample of the regioisomeric mixture of pyrazine *N*-oxides **24b(i)** and **24b(ii)** was refluxed in methanol (15 mL) for 4 h. After this time, the solvent was removed under reduced pressure and the residue purified by flash chromatography ($CHCl_3$:MeOH, 90:10), resulting in the elution of the 90 mg (49%) of the pyrazine 1-*N*-oxide regioisomer **28b(i)**, followed by 10 mg (5%) of a mixed fraction and finally elution of the pyrazine 4-*N*-oxide regioisomer **28b(ii)**, 50 mg (27%). Pyrazine 1-*N*-oxide regioisomer **28b(i)**: mp 109–113 °C; ^{1}H NMR ($CDCl_3$) **28b(i)** 0.95 (3H, t, J = 7.2), 1.41 (2H, sext, J = 7.4), 1.77 (2H, quint, J = 7.3), 2.43 (3H, s). 2.70 (2H, t, J = 7.3), 2.91 (3H, s), 5.01 (2H, s), 7.03–7.96 (9H, m), 8.04 (1H, s), 8.20 (1H, s). Anal. ($C_{27}H_{28}N_8O$) C, H, N. Pyrazine 4-*N*-oxide regioisomer **28b(ii)**: mp 208–212 °C; ^{1}H NMR ($CDCl_3$) **28b-(ii)** 0.92 (3H, t, J = 7.3), 1.39 (2H, sext, J = 7.6), 1.69 (2H, quint, J = 8.0), 2.47 (3H, s), 2.69 (2H, t, J = 8.2), 2.76 (3H, s), 5.1 (2H, s), 7.0 and 7.15 (2H and 2H, d, J = 8.21), 7.40–7.60 (6H, m), 7.98 (1H, s). Anal. ($C_{27}H_{28}N_8O$) C, H, N.

2-Butyl-5-(3-carbomethoxy-6-methylpyridin-2-yl)-1-[[2-(trimethylsilyl)ethoxy]methyl]-1*H*-imidazole (14b). Step 4. A 8.5 g (73%, 11.41 mmol) sample of stannylimidazole **10** was refluxed with 2.11 g (11.41 mmol) of 3-carbomethoxy-2-chloro-6-methylpyridine in dioxane (120 mL) with tetrakis(triphenylphosphine)palladium(0) (0.66 g, 0.57 mmol) and 2,6-di-*tert*-butyl-4-methylphenol (5 mg) for 5 h. The mixture was then partitioned between saturated sodium fluoride solution (70 mL) and ether (70 mL). The ether phase was separated, washed with brine (3 × 70 mL), and dried (Na_2SO_4), and solvent was removed under reduced pressure. The crude material was purified by flash chromatography ($CHCl_3$:MeOH, 95:5) to give 3.38g (72%) of **14b** as an oil: ^{1}H NMR ($CDCl_3$) −0.11 (9H, s), 0.73 (3H, t, J = 7.1), 0.96 (3H, t, J = 7.2), 1.45 (2H, sext, J = 7.5), 1.83 (2H, pent, J = 8.0) 2.6 (3H, s), 2.81 (2H, t, J = 8.0), 3.35 (2H, t, J = 7.1), 3.73 (3H, s), 5.56 (2H, s), 7.27 (1H, s), 7.14 (1H, d, J = 7.0), 7.93 (1H, d, J = 8.0).

2-Butyl-5-(3-carbomethoxy-6-methylpyridin-2-yl)-1*H*-imidazole (18b). Step 5. Method B. A 3 g (7.6 mmol) sample of **14b** was refluxed in MeOH (18 mL) and 7 M methanolic HCl (15 mL) for 3 h. Workup as previously described and purification of the crude material by filtration through silica ($CHCl_3$:MeOH, 97:3) gave 7.80 g (88%) of **18b** as a solid: mp 89–93 °C; ^{1}HMR ($CDCl_3$) 0.93 (3H, t, J = 7.2), 1.42 (2H, sext, J = 7.4), 1.78 (2H, pent, J = 7.5), 2.56 (3H, s), 2.76 (2H, d, J = 7.4), 3.91 (3H, s), 6.99 (1H, d, J = 8.0), 7.62 (1H, s), 7.91 (1H, d, J = 8.0).

2-Butyl-4-(3-carbomethoxy-6-methylpyridin-2-yl)-1-[[1-[1-(triphenylmethyl)1H-tetrazol5-yl][1,1′-biphenyl]-4-yl]methyl]-1*H*-imidazole (22b). Step 6. A 820 mg (3 mmol) sample of **18b** in DMF (25 mL) was reacted with sodium hydride (156 mg, 60% dispersion in oil, 3.9 mmol) followed by addition of **23** (2.3 g, 75%, 3.09 mmol) in DMF (35 mL). After stirring overnight the reaction mixture was quenched with ice/water and extracted with ethyl acetate (3 × 50 mL). The combined organic extracts were washed with water (2 × 50 mL) and then brine (50 mL). Drying over Na_2SO_4 and removal of solvent under reduced pressure gave a crude material which was purified by flash chromatography ($CHCl_3$:MeOH, 99:1) to give 1.26 g (56%) of **22b** as a colorless solid: mp 80–86 °C; ^{1}H NMR ($CDCl_3$) 0.89 (3H, t, J = 7.2), 1.35 (2H, sext, J = 7.4), 1.70 (2H + H_2O, br m), 2.53 (3H, s), 2.58 (2H, t, J = 7.8), 3.86 (3H, s), 4.94 (2H, s), 7.0 (1H, d, J = 8), 7.48 (1H, s), 7.68 (1H, d, J = 8), 6.83–7.98 (23H, m).

2-Butyl-4-(3-carbomethoxy-6-methylpyridin-2-yl)-1-[[2′-(1*H*-tetrazol-5-yl)[1,1′-biphenyl]-4-yl]methyl]-1*H*-imidazole (6b) was obtained from **22b** (350 mg, 0.47 mmol) by refluxing in methanol (40 mL) for 1 h. Removal of solvent under reduced pressure and crystallization of the residue from ether gave 200 mg (84%) of **6b**: mp 145–150 °C; ^{1}H NMR ($CDCl_3$) 0.91 (3H, t, J = 7.3), 1.41 (2H, sext, J = 7.6), 1.66 (2H, pent, J = 7.63), 2.37 (3H, s), 2.54 (2H, t, J = 7.2), 3.80 (3H, s), 5.0 (2H, s), 6.98 (1H, d, J = 8.3), 7.26 (1H, s), 7.70 (1H, d, J = 7.9), 6.83–7.68 (9H, m). Anal. ($C_{29}H_{29}N_7O_2$) C, H, N.

2-Butyl-4-(3-carbomethoxy-6-methyl-*N*-oxopyridin-2-yl)-1-[[2′-[1-(triphenylmethyl)-1*H*-tetrazol-5-yl][1,1′-biphenyl]-4-yl]methyl]-1*H*-imidazole (27b) was obtained by treating **22b** (1 g, 1.33 mmol) in CH_2Cl_2 (40 mL) with MCPBA (349 mg, 66%, 1.33 mmol) and stirring the reaction overnight at room temperature. The mixture was then washed with 0.1 N NaOH (3 × 40 mL) and the organic phase dried ($MgSO_4$). Removal of solvent under reduced pressure and purification of the residue by flash chromatography (CH_2Cl_2:acetone, 8:2) gave 200 mg (20%) of **27b** as a yellow resin: ^{1}H NMR ($CDCl_3$) 0.99 (3H, t, J = 7.13), 1.30 (2H, sext, J = 6.8), 1.74 (2H + H_2O, br m), 2.68 (3H, s), 2.76 (2H, d, J = 7.4), 3.91 (3H, s), 6.99 (1H, d, J = 8.0), 7.62 (1H, s), 7.91 (1H, d, J = 8.0).

2-Butyl-4-(3-carbomethoxy-6-methyl-*N*-oxopyridin-2-yl)-1-[[2′-(1*H*-tetrazol-5-yl][1,1′-biphenyl]-4-yl]methyl]-1*H*-imidazole (31b) was obtained by refluxing the compound **27b** (180 mg, 0.23 mmol) in methanol (30 mL) for 1 h.

Removal of solvent under reduced pressure and crystallization from ether gave **31b**, 104 mg (86%) as a yellow solid: mp 200–204 °C; ^{1}H NMR ($CDCl_3$) 0.98 (3H, t, J = 7.2), 1.43 (2H, sext, J = 7.6), 1.80 (2H, pent, J = 7.1), 2.61 (3H, s), 2.76 (2H, t, J = 7.3), 3.93 (3H, s), 5.0 (2H, s), 7.17 (1H, d, J = 7.9), 7.35 (1H, d, J = 7.9), 8.06 (1H, s), 7.13–8.09 (9H, m). Anal. ($C_{29}H_{29}N_7O_3$) C, H, N.

Pharmacology [^{3}H]A II Binding Assay. Rat adrenal cortex membranes were prepared according to Chang et al.[30] A II (1 μM) was used for the determination of nonspecific binding. Losartan (10^{-11}–10^{-4} M) was tested as a reference standard. The test compounds were dissolved in 100% DMSO at the concentration of 10^{-2} M and then diluted with assay buffer[31] and used in the assay in range of concentrations from 10^{-11}–10^{-4} M. For the assay, 50 μL of test compound were added into test tubes containing 100 μL of membrane suspension (0.05 mg of protein), 50 μL of [^{3}H]A II (Amersham, U.K., 1.2 nM, final concentration), and assay buffer in a final volume of 0.5 mL. After 60 min of incubation at 25 °C, the reaction was terminated by filtration under reduced pressure through glass fiber GF/B filters (presoaked for 3–5 h in 0.5% bovine serum albumin solution) using a Brandel cell harvester and washed rapidly three times with ice-cold Tris-HCl (50 mM, pH 7.4). The radioactivity was determined by scintillation counting using a Packard 2200 CA scintillation counter. The K_i values were determined using EBDA/LIGAND, a nonlinear iterative fitting program.[32]

A II-Induced Pressor Response in Conscious Normotensive Rats. Male Sprague–Dawley rats (Charles River, Calco, Italy) weighing 280–340 g were premedicated ip with fentanyl (0.024 mg kg^{-1}) plus fluanisone (1.2 mg kg^{-1}) (Hypnorm) and anesthetized with sodium pentobarbital (30–35 mg kg^{-1} iv). Polyethylene catheters were inserted into the left carotid artery and jugular vein and exteriorized behind the head through a single channel swivel (U. Danuso, Milan, Italy). The carotid catheter was connected to a Transpac II transducer (Abbott, Campoverde, Italy), and blood pressure and heart rate were recorded by a 7758 D polygraph (Hewlett-Packard). Data samples of variables were taken using an IDAS BM 9000 (Biomedica Mangoni, Pisa, Italy) coupled to a Compaq 386/20e computer. Eighteen hours after surgery, following an overnight fast with water ad libitum, A II (0.105 nmol kg^{-1} iv) was injected three times at 20 min intervals to establish the baseline response. Then the vehicle or compounds (2 μmol kg^{-1}) was administered orally by stomach tube, and A II bolus injections were performed every 15 min for the first hour and then every 30 min after that. The data were updated as the maximal inhibition of A II-induced pressor response and the duration of the effect (AUC).

Acknowledgment. We are grateful to Mr. M. Bennati, Mr. M. Bassoni (Chemistry), and Mr. M. Guelfi (Pharmacology) for their dedicated technical assistance given throughout the course of this work.

References

(1) Furakawa, Y.; Kishimoto, S.; Nishikawa, K. U.S. Patents 4,340,598 and 4,355,640, 1982.
(2) Duncia, J. V.; Carini, D. J.; Chiu, A. T.; Johnson, A. L.; Price, W. A.; Wong, P. C.; Wexler, R. R.; Timmermans, P. B. M. W. M. The discovery DuP-753, A Potent Orally Active Nonpeptide Angiotensin II Antagonist. *Med. Res. Rev.* **1992**, *12*, 149–191.
(3) Mantlo, N. B.; Chakravarty, P. K.; Ondeyka, D. L.; Siegl, P. K. S.; Chang, R. S.; Lotti, V. J.; Faust, K. A.; Chen, T. B.; Schorn, T. W.; Sweet, C. S.; Emmert, S. E.; Patchett, A. A.; Greenlee, W. J. Potent Orally Active Imidazo[4,5-b]pyridine Based Angiotensin II Receptor Antagonists. *J. Med. Chem.* **1991**, *34*, 2919–2922.
(4) Olins, G. M.; Corpus, V. M.; McMahon, E. G.; Palomo, M. A.; Schuh, J. R.; Blehm, P. J.; Huang, H. C.; Reitz, D. B.; Manning, R. E.; Blaine, E. H. In Vitro pharmacology of a Non-peptidic Angiotensin II Receptor Antagonist, S.C.-51316. *J. Pharmacol. Exp. Ther.* **1992**, *261*, 1037–1043.
(5) Chang, L. L.; Ashton, W. T.; Flanagan, H. L.; Strelitz, R. A.; McCoss, M.; Grenlee, W. J.; Chang, R. S. L.; Lotti, V. J.; Faust, K. A.; Chen, T. B.; Bunting, P.; Zingaro, G. J.; Kivlighn, S. D.; Siegl; P. K. S. Triazolinones as Nonpeptide Angiotensin II Antagonists I. Synthesis and Evaluation of Potent 2,4,5-Trisubstituted Triazolinones. *J. Med. Chem.* **1993**, *36*, 2558–2568.
(6) Cazaubon, C.; Gougat, J.; Bousquet, F.; Girandou, P.; Gayraud, R.; Lacour, C.; Raccon, A.; Galindo, G.; Barthélémy, G.; Gautret, B.; Bernhart, G.; Perreaut, P.; Brelière, J. C.; Le Fur, G.; Nisato, D. Pharmacology of a Non-peptide Angiotensin II Receptor Antagonist SR 47436. *J. Pharmacol. Exp. Ther.* **1993**, *265*, 826.
(7) Veyama, N.; Yanagisawa, T.; Baba, H.; Kuroiwa, M.; Hayashi, H.; Sonegawa, M.; Tomiyama, T. Cycloheptimidazole Based Angiotensin II Receptor Antagonists. 4,5,6,7-Tetrahydro-8-carboxy-methyliene cycloheptimidazoles. *Bioorg. Med. Chem. Lett.* **1994**, *4*, 1637.
(8) (a) Oldham, D. A.; Allott, C. P.; Major, J. S.; Pearce, M. J.; Roberts, D. A.; Russel, S. T. ICI D8731 A Novel Potent Orally Effective Angiotensin II Antagonist. *Br. J. Pharmacol.* **1992**, Suppl., 83 p. (b) Bradbury, R. N.; Allot, C. P.; Dennis, M.; Girdwood, J. A.; Kenny, P. W.; Major, J. S.; Oldham, A. A.; Ratcliffe, A. N.; Kenny, J. E.; Roberts, D. A.; Robins, P. J. New Non-peptide Angiotension II Receptor Antagonist. Synthesis, Biochemical Properties and Structure-Activity Relationships of 2-Alkyl-4-(biphenylmethoxy) pyridine Derivatives. *J. Med. Chem.* **1993**, *36*, 1245–1254.
(9) Winn, M.; De, B.; Zydowsky, T. M.; Altenbach, R. J.; Basha, F. Z.; Boyd, S. A.; Brune, M. E.; Buckner, S. A.; Crowell, De. A.; Drizin, I.; Hancock, A. A.; Jae, H. S.; Ketser, J. A.; Lee, J. Y.; Mantei, R. A.; Marsh, K. C.; Novosad, E. I.; Oheim, K. W.; Rosenberg, S. H.; Shiosaki, K.; Sorensen, B. K.; Spira, K.; Sullivan, G. M.; Tasker, A. S.; Von Geldern, T. W.; Warner, R. B.; Opgenorth, T. J.; Kerkman, D. J.; De Bernardis, J. F. 2-(Alkylamino)nicotinic Acid and Analogs. Potent Angiotensin II Antagonists. *J. Med. Chem.* **1993**, *36*, 2676–2688.
(10) Ellingboe, J. W.; Antane, M.; Nguyen, T. T.; Collini, M. D.; Antane, S.; Bender, R.; Hartupee, D.; White, V.; McCallum, J.; Park, C. H.; Russo, A.; Osler, M. B.; Wojdan, A.; Dinish, J.; Ho, D. M.; Bagli, J. F. Pyrido[2,3-*d*]pyrimidine Angiotensin II Antagonists. *J. Med. Chem.* **1994**, *37*, 542–550.
(11) Bühlmayer, P.; Furet, P.; Criscione, L.; De Gasparo, M.; Whitebread, S.; Schmidlin, T.; Lattmann, R.; Wood, J. Valsartan. A Potent Orally Active Angiotensin II Antagonist Developed From The Structurally New Amino Acid Series. *Bioorg. Med. Chem. Lett.* **1994**, *4*, 29–34.
(12) (a) Hodges, J. C.; Hamby, J. M.; Blankley, J. Angiotensin II Receptor Binding Inhibitors, Review Article, *Drugs Future* **1992**, *17* (7), 575–593. (b) Timmermans, P. B. M. W. M.; Wong, P. C.; Chiu, A. T.; Herblin, W. F. Non-Peptide Angiotensin II Receptor Antagonists. *Trends Pharmacol. Sci.* **1991**, *12*, 55–62. (c) Chiu, A. T.; Carini, D. J.; Duncia, J. V. DuP 532: A Second Generation of Non-Peptide Angiotensin II Receptor Antagonists, *Biochem. Biophys. Res. Commun.* **1991**, *177*, 209–217.
(13) Keenan, R. M.; Weinstock, J.; Finkelstein, J. A.; Franz, R. G.; Gaitanopoulos, D. E.; Girard, G. R.; Hill, D. T.; Morgan, T. M.; Samanen, J. M.; Hempel, J.; Eggleston, D. S.; Aiyar, N.; Griffin, E.; Ohlstein, E. H.; Stack, E. J.; Weidley, E. F.; Edwards, R. Imidazole-5-acrylic Acids: Potent Non-peptide Angiotensin II Receptor Antagonists, Designed Using A Novel Peptide Pharmacophore Model. *J. Med. Chem.* **1992**, *35*, 3858–3872.
(14) 5-Bromo-4-carbomethoxy-2-methylpyrimidine: Budesinsky, Z., Derivatives of 2-methylpyrimidine. *Collect. Czech. Chem. Commun.* **1949**, *14*, 223–235; *Chem. Abstr.* **1950**, *44*, 1516.
(15) (a) 2-Bromo-3-carbomethoxypyrazine: Ellingson, R. C.; Henry, R. L.; Pyrazine Chemistry. IV. Bromination of 2-amino-3-carbomethoxypyrazine. *J. Am. Chem. Soc.* **1949**, *75*, 2798–2800. (b) Sherlock, M. N. U.S. Patent, 4,492,702, 1985.
(16) Methyl 3-chloropyridazine-6-carboxylate: Barlin, G. B.; Yoot-Yap, C. Some 3-halogenopyridazines. *Aust. J. Chem.* **1977**, *30*, 2319–2322.
(17) Methyl-2-chloronicotinate: Robison, M. M.; Robison, B. L. 7-Azaindole I. Synthesis and Conversion to 7-Azatryptophan and Other Derivatives. *J. Am. Chem. Soc.* **1955**, *77*, 457–460.
(18) Methyl-6-bromopicolinate: Gilman, H.; Spatz, S. M. Pyridinylithium Compounds. *J. Org. Chem.* **1951**, *16*, 1485.
(19) Methyl 5-bromopicolinate: (a) Paul, J. S.; Sheehan, J. T.; U.S. Patent 3,553,203, 1971. (b) Blank, B.; Di Tullio, N. W.; Miao, C. K.; Owings, F. F.; Gleason, J. G.; Ross, S. T.; Berkhoff, C. E.; Saunders, H. L.; De Large, J.; Lapière, C. L. Mercaptopyridinecarboxylic Acids, Synthesis and Hypoglycemic Activity. *J. Med. Chem.* **1974**, *17*, 1065–1071.
(20) Methyl 3-bromonicotinate: Bachmann, G. C.; Micucci, D. D. Vinylpyridines and Vinylquinoines, *J. Am. Chem. Soc.* **1948**, *70*, 2381–2384.
(21) Methyl 5-bromoisonicotinate: De Jardis, J. V.; Lapière, C. L. New Syntheses of 3-hydroxypyridine 4-carboxylic and 3-amino pyridine-4-carboxylic acids. *Bull. Chim. Soc. Fr.* **1976**, 530–532.

(22) Duncia, J. V.; Chiu, A. T.; Carini, D. J.; Gregory, G. B.; Johnson, A. L.; Price, W. A.; Wells, G. J.; Wong, P. C.; Calabrese, J. C.; Timmermans, P. B. M. W. M. The Discovery of Potent Non-peptide Angiotension II Receptor Antagonists: A New Class of Potent Antihypertensives. *J. Med. Chem.* **1990**, *33*, 1312–1327.
(23) (a) Scrocco, E.; Tomasi, J. In *Topics in Current Chemistry*; no. 42; Springer Verlag: Berlin, 1973; p 95. (b) Ghio, G.; Tomasi, J. *Theor. Chim. Acta* **1973**, *30*, 151. (c) Scrocco, E.; Tomasi, J. *Adv. Quant. Chem.* **1978**, *11*, 11S. (d) Politzer, P., Truhlar, D. G., Eds. *Chemical Applications of Atomic and Molecular Eletrostratic Potentials*; Plenum Press: New York, 1981.
(24) Frish, M. J.; Trucks, G. W.; Head-Gordon, M.; Gill, P. M. W.; Wong, M. W.; Foresman, J. B.; Johnson, B. G.; Schlegel, H. B.; Robb, M. A.; Replogle, E. S.; Gomperts, R.; Andres, J. L.; Raghavackari, K.; Binkley, J. S.; Gonzales, C.; Martin, R. L.; Fox, D. J.; Defrees, D. J.; Baker, J.; Stewart, J. J. P.; Pople, J. A. *Gaussian 92, Revision A*; Gaussian, Inc.: Pittsburg, PA, 1992.
(25) Alagona, G.; Ghio, C. *J. Mol. Struct. (THEOCHEM)* **1992**, *256*, 187.
(26) Stradler, C. D.; Sigal, I. S.; Dixon, R. A. F. *Am. J. Respir. Cell. Mol. Biol.* **1989**, *1*, 81.
(27) Wong, P. C.; Price, W. A.; Chiu, A. T.; Duncia, J. V.; Carini, D. J.; Wexler, R. R.; Johnson, A. L.; Timmermans, P. B. M. W. M. Non-peptide Angiotensin II Receptor Antagonists XI. Pharmacology of EXP-3174: An Active Metabolite of Dup 753, An Orally Active Antihypertensive Agent. *J. Pharmacol. Exp. Ther.* **1990**, *255*, 211–219.
(28) SURFER, Golden Software Inc., P.O. Box 281, Golden, CO 80402.
(29) Whitten, J. P.; Matthews, J. P.; McCarthey, J. R. [2-(trimethylsilyl)etoxy]methyl (SEM) As A Novel and Effective Imidazole and Fused Aromatic Imidazole Protecting Group. *J. Org. Chem.* **1986**, *51*, 1891–1894.
(30) Chang, R. S. L.; Lotti, V. J.; Chen, T. B.; Faust, K. A. Two Angiotensin II Binding Sites In Rat Brain Revealed Using [^{125}I]-Sar^{1}, Ile^{8}-Angiotensin II and Selective Non-peptide Antagonists. *Biochem. Biophys. Res. Commun.* **1990**, *171*, 813–817.
(31) Renzetti, A. R.; Cucchi, P.; Guelfi, M.; Salimbeni, A.; Subissi, A.; Giachetti, A. Pharmacology of LR-B/057: A Novel Orally Active AT_1 Receptor Antagonist. *J. Cardiovasc. Pharmacol.* **1995**, *25*, 354–360.
(32) McPherson, G. A. Analysis of Radioligand Binding Experiments: A Collection of Computer Programs for IBM PC. *J. Pharmacol. Methods* **1985**, *14*, 213–228.

JM950076J